Zinc(II), Copper(II) and Silver(I) Salicylate-Metronidazole Complexes as novel Antimicrobial Agents

Laura Contini,[a] Raymond J. Turner[b,*] and Fabrizia Grepioni[a,*]

[a]Dipartimento di Chimica "Giacomo Ciamician", Università di Bologna, via Gobetti 85, 40129 Bologna, Italy

[b]Department of Biological Sciences, University of Calgary, Canada

Electronic Supplementary Information (13 pages)

1. Powder X-ray diffraction.....Page 2

2. Crystallographic tables .....Page 5

3. DSC and TGA .....Page 8

4. Antimicrobial efficacy.....Page 9

5. Hirshfeld surface analysis.....Page 10

6. References .....Page 13

1. Powder X-ray diffraction

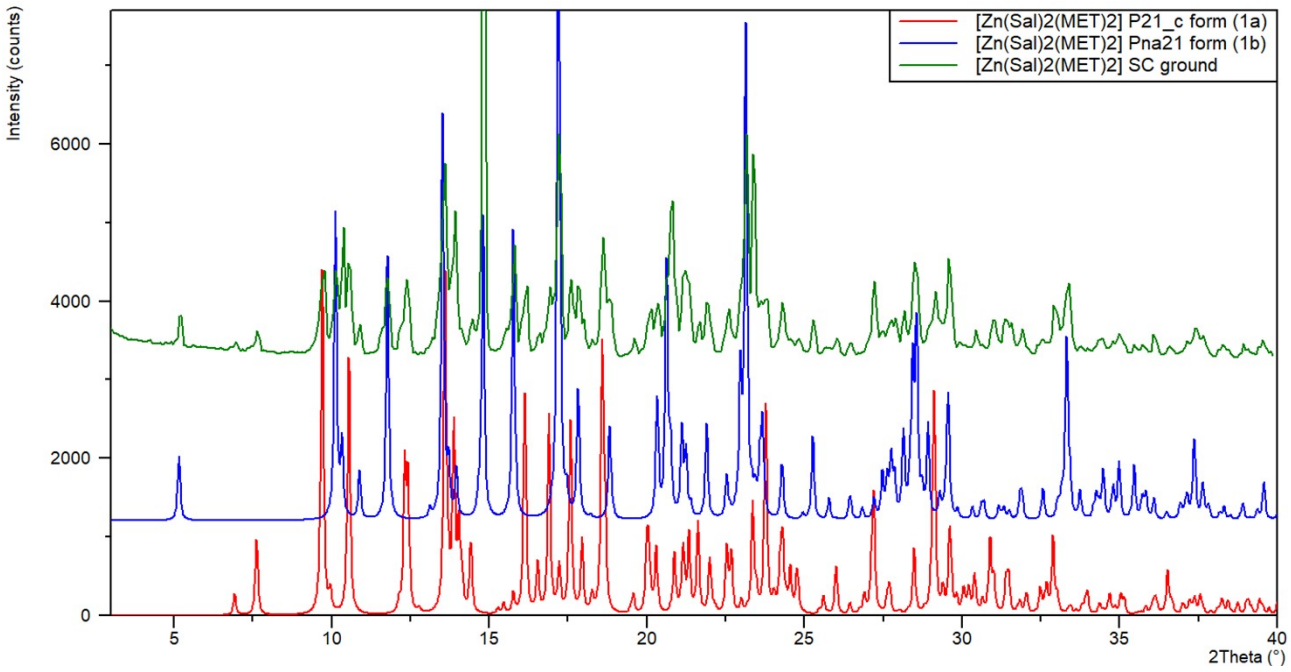

Figure ESI-1. Comparison between the experimental PXRD patterns obtained by grinding single crystals of $[Zn(Sal)_2(MET)_2]$ (**1a,** green) and the calculated ones of the monoclinic (**1a**, red) and orthorhombic (**1b**, blue) forms.

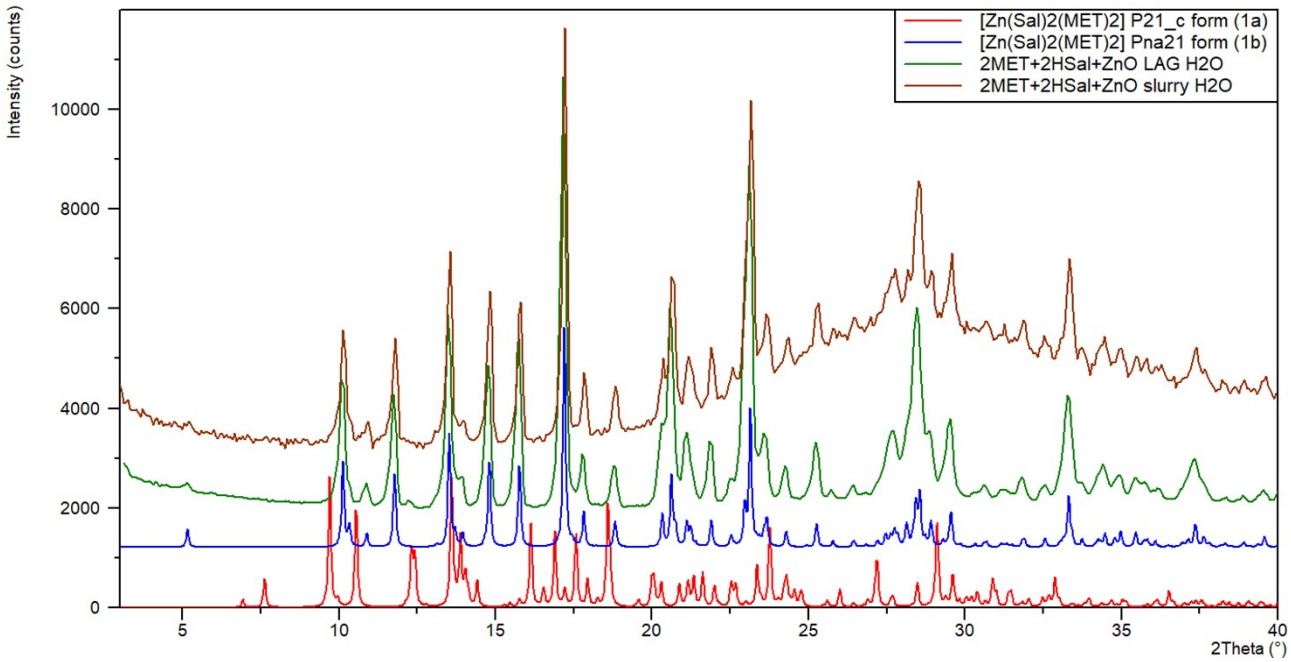

Figure ESI-2. Comparison between the experimental PXRD patterns for $[Zn(Sal)_2(MET)_2]$ (**1b**) obtained via LAG (green) and slurry (brown) using salicylic acid and ZnO as starting materials, and the calculated ones of the monoclinic (**1a**, red) and orthorhombic (**1b**, blue) forms.

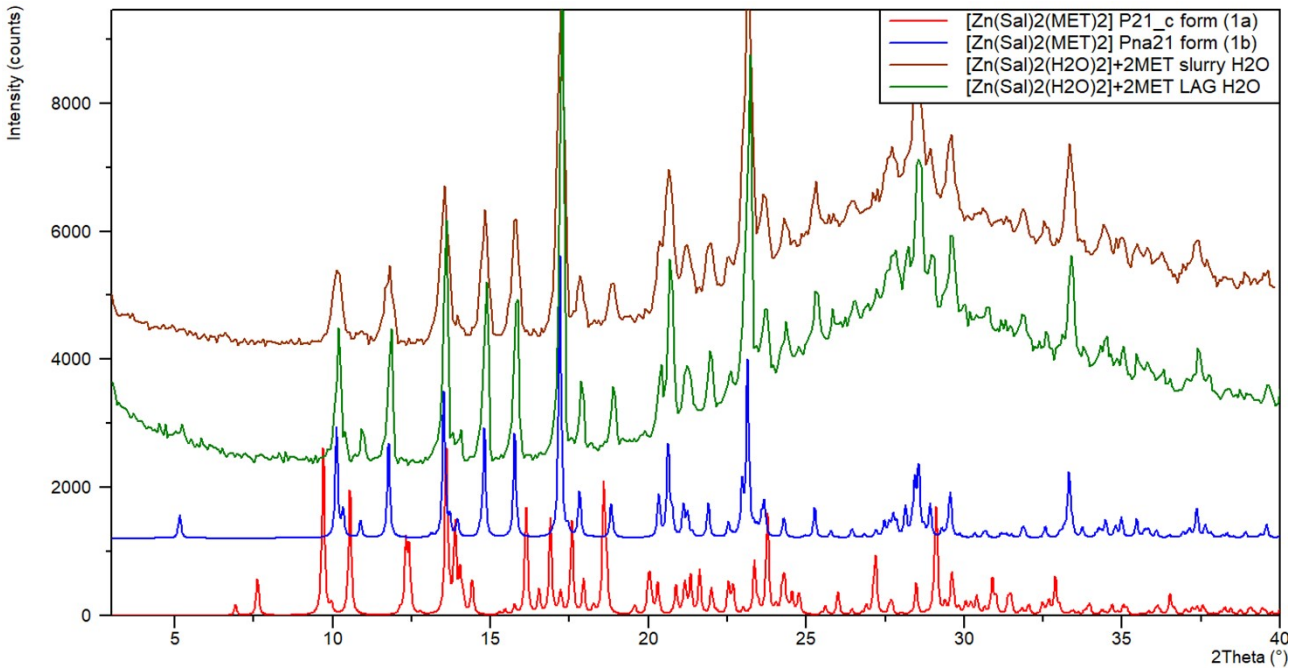

Figure ESI-3. Comparison between the experimental PXRD patterns for $[Zn(Sal)_2(MET)_2]$ (**1b**) obtained via LAG (green) and slurry (brown) using $[Zn(Sal)_2(H_2O)_2]$ as starting material, and the calculated ones of the monoclinic (**1a, red**) and orthorhombic (**1b**) forms.

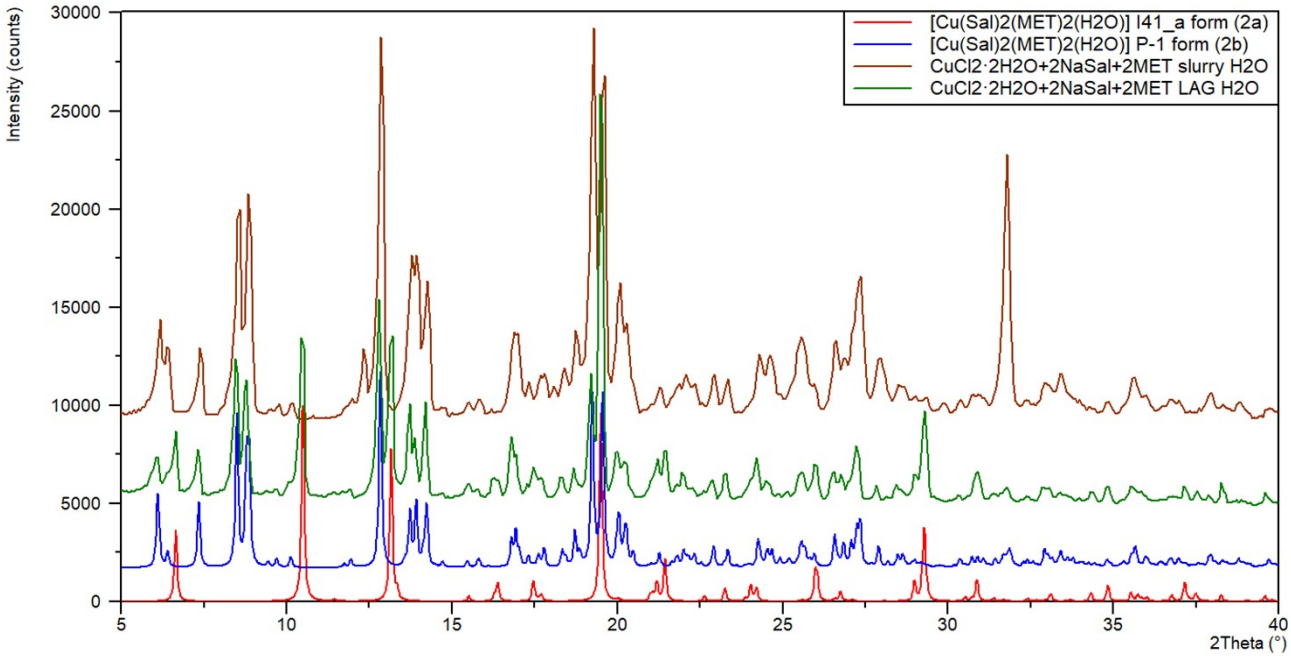

Figure ESI-4. Comparison between the experimental PXRD patterns for $[Cu(Sal)_2(MET)_2]$ (**2**) obtained via LAG (green) and slurry (brown) using sodium salicylate and $CuCl_2{\cdot}2H_2O$ as starting materials, and the calculated ones of the tetragonal (**2a**) and triclinic (**2b**) forms.

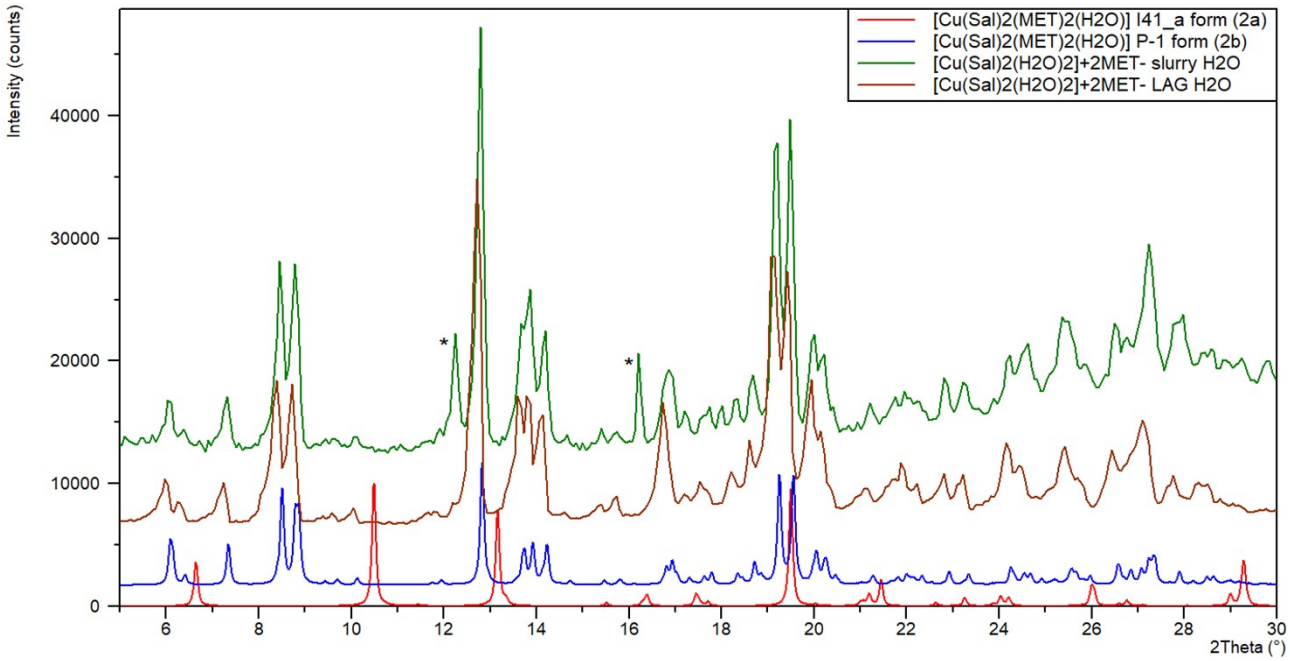

Figure ESI-5. Comparison between the experimental PXRD patterns for $[Cu(Sal)_2(MET)_2]$ (**2**) obtained via LAG (brown) and slurry (green) using $[Cu(Sal)_2(H_2O)_2]$ as starting materials, and the calculated ones of the tetragonal (**2a**) and triclinic (**2b**) forms.

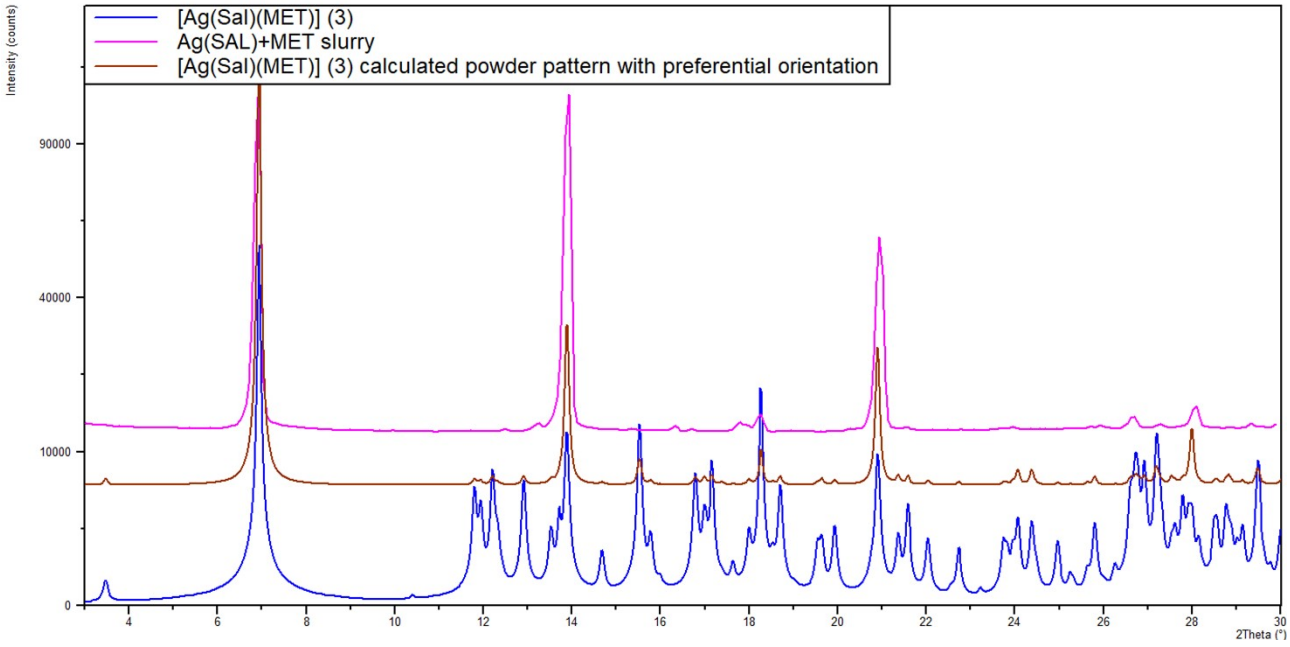

Figure ESI-6. Comparison between the experimental PXRD pattern for [Ag(Sal)(MET)] (**3**) obtained via slurry (brown) and the calculated one (blue). Due to the presence of preferential orientation in the experimental sample, the calculated powder pattern where the presence of preferential orientation is accounted for is also present in the plot (brown).

2. Crystallographic tables

a. $[Zn(Sal)_2(MET)_2]$

Table ESI-1. Crystallographic data and details of measurement at 293 K for $[Zn(Sal)_2(MET)_2]$ Form I (**1a**) and Form II (**1b**).

	$[Zn(Sal)_2(MET)_2]$ (**1a**)	$[Zn(Sal)_2(MET)_2]$ (**1b**)
Chemical formula	$C_{26}H_{28}N_6O_{12}Zn$	$C_{26}H_{28}N_6O_{12}Zn$
Formula weight/ g mol^{-1}	681.91	681.91
Crystal system	monoclinic	orthorombic
Space group	$P2_1/c$	$Pna2_1$
a / Å	8.8818(2)	34.2296(10)
b / Å	25.5076(8)	8.3588(3)
c / Å	13.0252(3)	10.1499(3)
α / °	90	90
β / °	92.435(2)	90
γ / °	90	90
Volume /Å^3	2948.24(13)	2904.07(16)
Z	4 (Z' =1)	4 (Z' =1)
d_{calc} / g·cm^{-3}	1.536	1.560
μ / mm^{-1}	0.907	0.921
Refls. measd./unique	12622/5775	12074/ 5712
R_{int}	0.0266	0.0293
Goodness-of-fit on F^2	1.045	1.088
R_1 [I >2σ (I)]	0.0453	0.0477
wR_2 [all data]	0.0919	0.0908
CCDC number	2448808	2448811

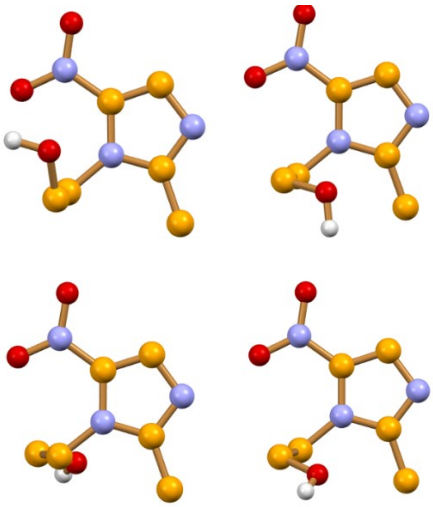

Figure ESI-7. Conformation of the MET ligands in $[Zn(Sal)_2(MET)_2]$ Form I (**1a**) (top) and Form II (**1b**) (bottom).

b. $[Cu(Sal)_2(MET)_2(H_2O)]$

Table ESI-2. Crystallographic data and details of measurement at 293 K for $[Cu(Sal)_2(MET)_2(H_2O)]$ Form I (**2a**) and Form II (**2b**).

	$[Cu(Sal)_2(MET)_2(H_2O)]$ (**2a**)	$[Cu(Sal)_2(MET)_2(H_2O)]$ (**2b**)
Chemical formula	$C_{26}H_{32}N_6O_{14}Cu$	$C_{26}H_{32}N_6O_{14}Cu$
Formula weight	716.11	716.11
Crystal system	tetragonal	triclinic
Space group	$I4_1/a$	P-1
a / Å	15.2859(3)	14.4255(7)
b / Å	15.2859(3)	14.5018(6)
c / Å	26.8974(9)	15.2572(7)
α / °	90	71.910(4)
β / °	90	87.960(4)
γ / °	90	89.334(4)
Volume /Å^3	6284.8(3)	3032.1(2)
Z	8 (Z' =1)	4 (Z' =2)
d_{calc} / g·cm^{-3}	1.514	1.529
μ / mm^{-1}	0.773	0.797
Refls. measd./unique	10320/3640	26129/13981
R_{int}	0.0544	0.0434
Goodness-of-fit on F^2	1.033	1.058
R_1 [I >2σ (I)]	0.0592	0.0593
wR_2 [all data]	0.1313	0.1495
CCDC number	2448810	2448809

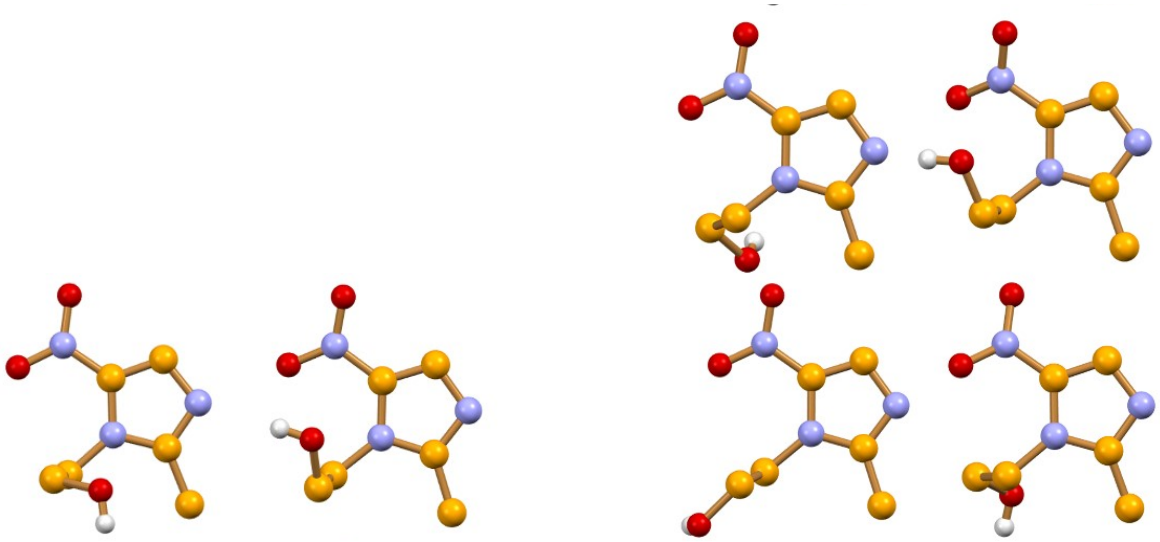

Figure ESI-8. Conformation of the MET ligands in $[Cu(Sal)_2(MET)_2(H_2O)]$ Form I (**2a**) (left) and Form II (**2b**) (right).

c. [Ag(Sal)(MET)]

Table ESI-3. Crystallographic data and details of measurement at 293 K for [Ag(Sal)(MET)] (**3**).

	[Ag(Sal)(MET)] (**3**)
Chemical formula	$C_{13}H_{14}O_6N_3Ag$
Formula weight	416.13
Crystal system	monoclinic
Space group	$P2_1/c$
a / Å	7.4945(3)
b / Å	7.4847(2)
c / Å	50.9813(19)
α / °	90
β / °	91.718(3)
γ / °	90
Volume /Å^3	2858.46(17)
Z	8 (Z' =2)
d_{calc} / g·cm^{-3}	1.934
μ / mm^{-1}	1.448
Refls. measd./unique	12721/6639
R_{int}	0.0423
Goodness-of-fit on F^2	1.137
R_1 [I >2σ (I)]	0.0657
wR_2 [all data]	0.1227
CCDC number	2448812

3. DSC and TGA

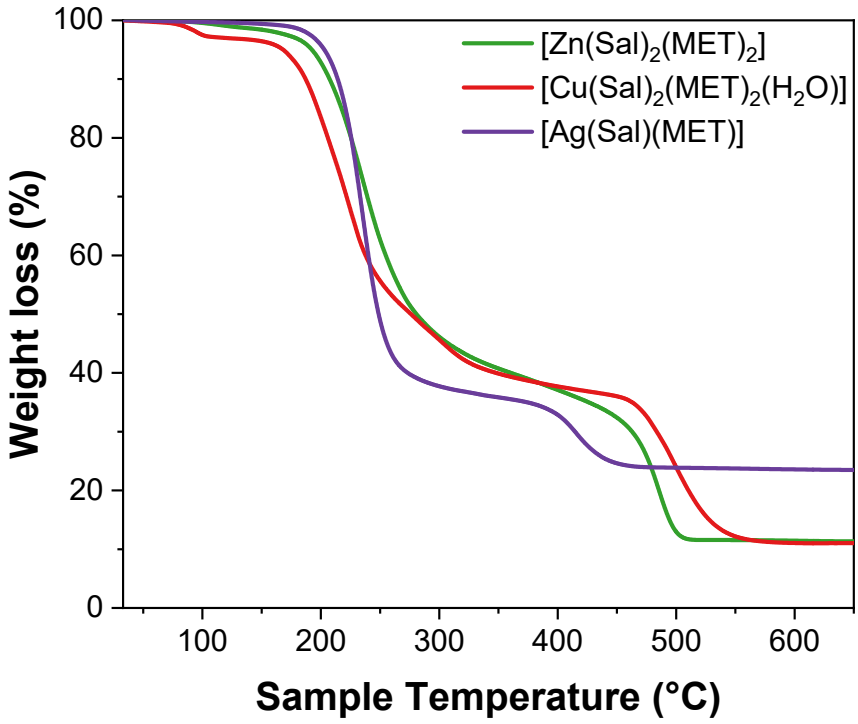

Figure ESI-9. TGA trace for $[Zn(Sal)_2(MET)_2]$ (**1b**, green), $[Cu(Sal)_2(MET)_2(H_2O)]$ (**2b**, red) and [Ag(Sal)(MET)] (**3**, purple).

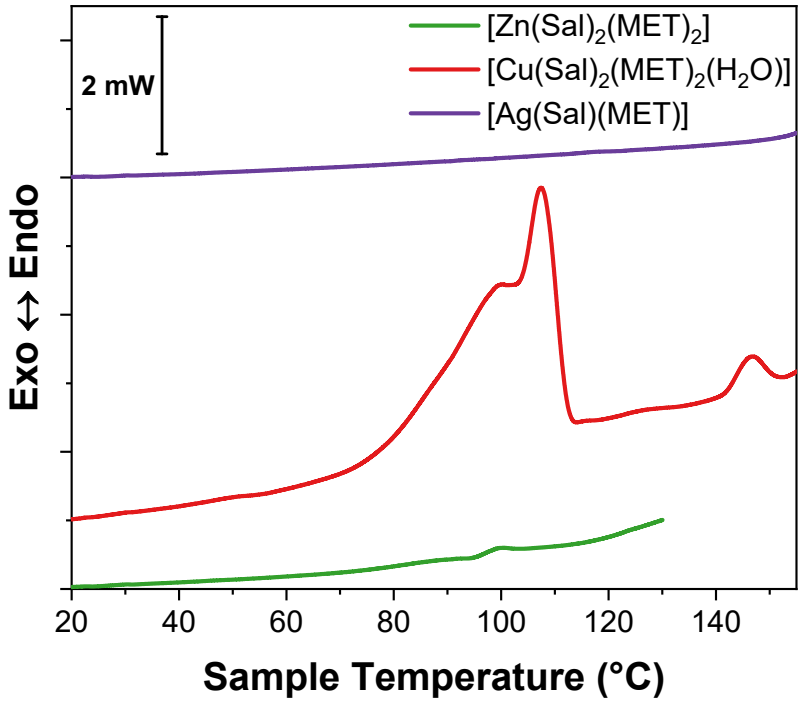

Figure ESI-10. DSC trace for $[Zn(Sal)_2(MET)_2]$ (**1b**, green), $[Cu(Sal)_2(MET)_2(H_2O)]$ (**2b**, red) and [Ag(Sal)(MET)] (**3**, purple).

4. Antimicrobial efficacy

Table ESI-4. Minimum inhibitory concentration (MIC). Concentrations are expressed in mM (mmol/L). If no end point was observed in the concentration range tested, -- was used.

Pathogen	MET	NaSal	$[Zn(Sal)_2(H_2O)_2]$	$[Cu(Sal)_2(H_2O)_2]$	[Ag(Sal)]
E. coli	14 ± 5	--	1.8 ± 0.7	2.7 ± 0	0.03 ± 0.01
P. aeruginosa	86 ± 19	--	4 ± 1	7 ± 2	0.08 ± 0.03
S. aureus	30 ± 15	--	1.2 ± 0.3	2.7 ± 0	0.08 ± 0.03
S. epidermidis	4 ± 2	--	0.67 ± 0	2.7 ± 0	0.08 ± 0.03

Table ESI-5. Minimum inhibitory concentration (MIC). Concentrations are expressed in mM (mmol/L). If no end point was observed in the concentration range tested, -- was used.

Pathogen	$[Zn(Sal)_2(MET)_2]$	$[Cu(Sal)_2(MET)_2(H_2O)]$	[Ag(Sal)(MET)]
E. coli	2.0 ± 0.7	1.9 ± 0.7	0.038 ± 0
P. aeruginosa	3 ± 1	2.9 ± 0	0.07 ± 0.02
S. aureus	1.4 ± 0.3	2.2 ± 0.7	0.09 ± 0.03
S. epidermidis	0.9 ± 0.3	1.9 ± 0.7	0.09 ± 0.03

Table ESI-6. Minimum bactericidal concentration (MBC). Concentrations are expressed in mM (mmol/L). If no end point was observed in the concentration range tested, -- was used.

Pathogen	MET	NaSal	$[Zn(Sal)_2(H_2O)_2]$	$[Cu(Sal)_2(H_2O)_2]$	[Ag(Sal)]
E. coli	--	--	5 ± 1	4 ± 1	0.07 ± 0.02
P. aeruginosa	--	--	5.33 ± 0	4 ± 1	0.5 ± 0.2
S. aureus	--	--	3 ± 1	5.35 ± 0	0.1 ± 0.4
S. epidermidis	6 ± 1	--	2.67 ± 0	5.35 ± 0	0.3 ± 0.1

Table ESI-7. Minimum bactericidal concentration (MBC). Concentrations are expressed in mM (mmol/L). If no end point was observed in the concentration range tested, -- was used.

Pathogen	$[Zn(Sal)_2(MET)_2]$	$[Cu(Sal)_2(MET)_2(H_2O)]$	[Ag(Sal)(MET)]
E. coli	2.7 ± 0.6	2.4 ± 0.7	0.04 ± 0.01
P. aeruginosa	--	2.9 ± 0	0.06 ± 0
S. aureus	2.2 ± 0.8	--	0.14 ± 0.05
S. epidermidis	2.0 ± 0.8	2.9 ± 0	0.24 ± 0.03

Table ESI-8. Fractional inhibitory concentration index (FIC index)

	MET + $[Zn(Sal)_2(H_2O)_2]$	MET + $[Cu(Sal)_2(H_2O)_2]$	MET + [Ag(Sal)]
P. aeruginosa	0.42 ± 0.09	0.7 ± 0.3	0.4 ± 0.2
S. epidermidis	1.1 ± 0.3	1.0 ± 0.3	0.8 ± 0.3

5. Hirshfeld surface analysis

Table ESI-9. Fingerprint plot and Hirshfeld surfaces (mapped over d_{norm}) of the complexes studied in this work.

	Structure	d_{norm} (front)	d_{norm} (back)	Fingerprint
1a	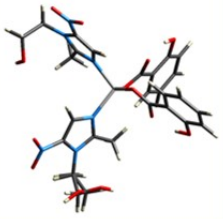	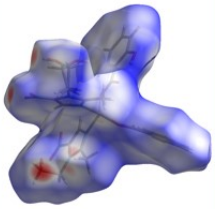	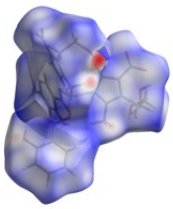	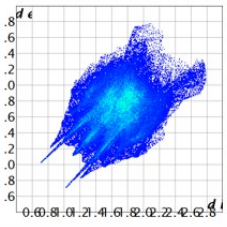
1b	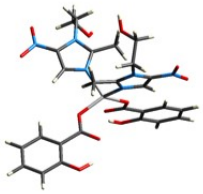	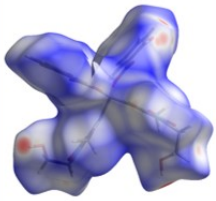	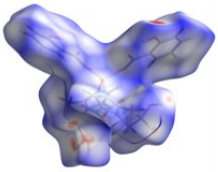	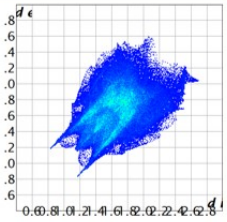
2a	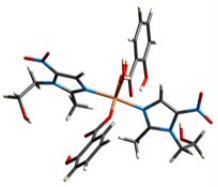	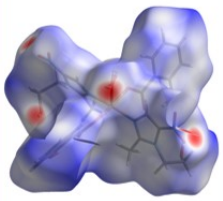	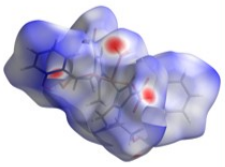	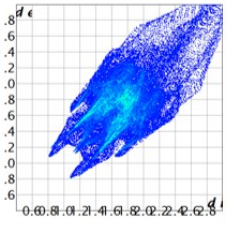
2b	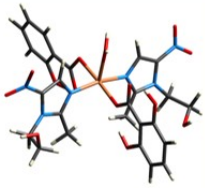 Fragment 1	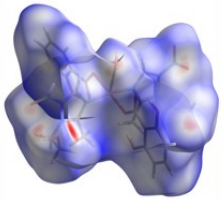	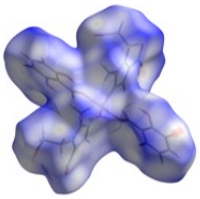	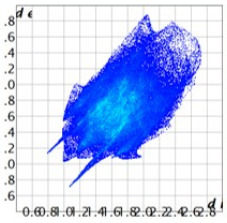
	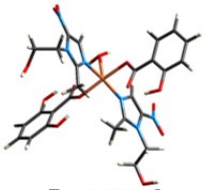 Fragment 2	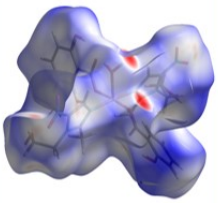	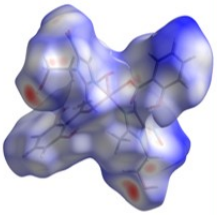	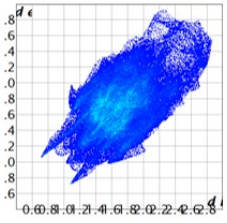
3	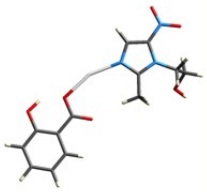 Fragment 1	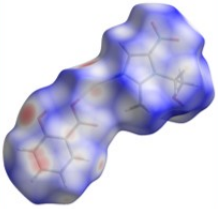	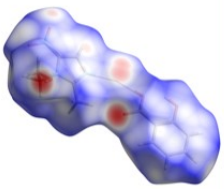	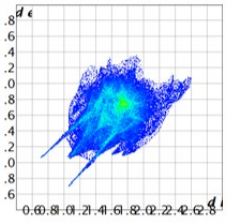
	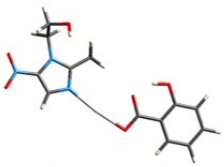 Fragment 2	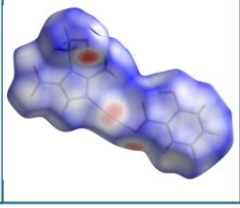	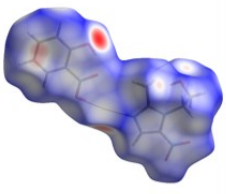	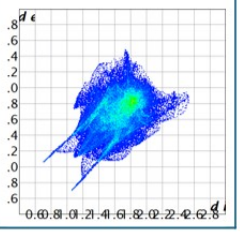

Table ESI-10. Hirshfeld surfaces of the complexes studied in this work mapped over curvedness.

	Curvedness (front)	Curvedness (back)	Globularity:	Asphericity:
1a	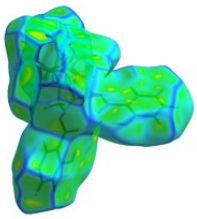	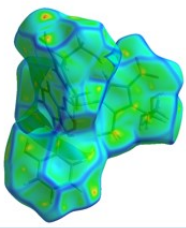	0.649	0.007
1b	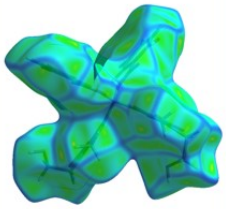	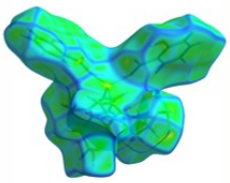	0.640	0.010
2a	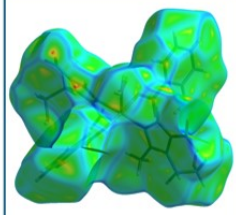	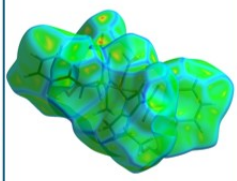	0.652	0.067
2b	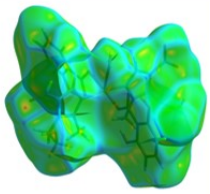 Fragment 1 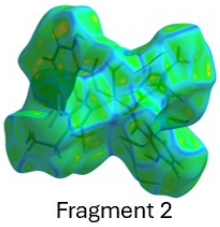 Fragment 2	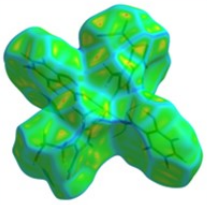 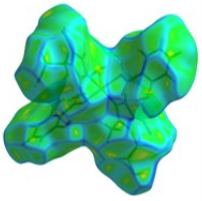	0.647 0.647	0.068 0.068
3	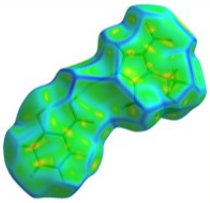 Fragment 1 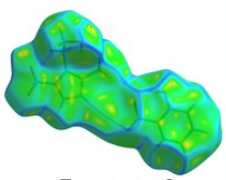 Fragment 2	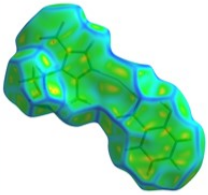 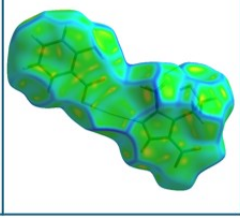	0.702 0.710	0.387 0.405

The intermolecular interactions within the crystal packing of complexes **1-3** were assessed by Hirshfeld surface analysis and 2D fingerprint plot calculations. Calculations were conducted with the CrystalExplorer software (version 21.5, revision 608bb31) using TONTO.[1–3] Analysis of Hirshfeld surfaces enables the possibility to visualize the intermolecular interaction within the crystal. The normalized contact distance (d_{norm}) is mapped onto the Hirshfeld surface and is reported in **Table ESI-9**. Red spots indicate close contacts between donor and acceptor atoms, with the intensity of the colour increasing as the atoms approach each other. Visualization of intermolecular interactions present in the molecular crystals is reported in the fingerprint plots (**Table ESI-9**). The globularity of all compounds studied is <1, indicating that all compounds have a non-spherical, more structured molecular shape (**Table ESI-10**). Similar consideration could be retrieved from the value of the asphericity parameter, which reflects the degree of anisotropy (**Table ESI-10**).[4]

6. References

1 S. L. Tan, M. M. Jotani and E. R. T. Tiekink, *Acta Cryst E*, 2019, 75, 308–318.

2 C. F. Mackenzie, P. R. Spackman, D. Jayatilaka and M. A. Spackman, *IUCrJ*, 2017, 4, 575–587.

3 P. R. Spackman, M. J. Turner, J. J. McKinnon, S. K. Wolff, D. J. Grimwood, D. Jayatilaka and M. A. Spackman, *J Appl Cryst*, 2021, 54, 1006–1011.

4 E. Macedi, P. Rossi, M. Formica, L. Giorgi, M. Lippi, R. Montis, D. Paderni, P. Paoli and V. Fusi, *Journal of Molecular Structure*, 2024, 1299, 137146.